Environment International 130 (2019) 104951

Contents lists available at ScienceDirect

Environment International

journal homepage: www.elsevier.com/locate/envint

Modified Palmer Drought Severity Index: Model improvement and application

Huiqian Yu[a,b,c,f], Qiang Zhang[a,b,c,f,*], Chong-Yu Xu[d], Juan Du[a,b,c,f], Peng Sun[e], Pan Hu[a,b,c,f]

[a] Key Laboratory of Environmental Change and Natural Disaster, Ministry of Education, Beijing Normal University, Beijing 100875, China
[b] Faculty of Geographical Science, Academy of Disaster Reduction and Emergency Management, Ministry of Education, Ministry of Emergency Management, Beijing Normal University, Beijing 100875, China
[c] State Key Laboratory of Earth Surface Processes and Resources Ecology, Beijing Normal University, Beijing 100875, China
[d] Department of Geosciences, Oslo University, Blindern, 0316, Oslo, Norway
[e] College of Territorial Resource and Tourism, Anhui Normal University, Anhui 241002, China
[f] Center for Human-Environment System Sustainability (CHESS), State Key Laboratory of Earth Surface Processes and Resource Ecology (ESPRE), Beijing Normal University, Beijing 100875, China

ARTICLE INFO

Handling Editor: Xavier Querol

Keywords:
Drought monitoring
SPI
SPEI
sc-PDSI
MPDSI
Irrigation

ABSTRACT

Monitoring of droughts is the first step into human adaptation and related management of drought hazards. Therefore, drought index is critical in drought monitoring practice. However, the standing drought indices include no information about agricultural irrigation. In this case, based on the Palmer Drought Severity Index (PDSI) and the Self-Calibrating Palmer Drought Severity Index (sc-PDSI), here we proposed the Modified Palmer Drought Severity Index (MPDSI) by considering agricultural irrigation such as irrigation quotas and soil water deficits. We compared changes of droughts monitored by MPDSI and other drought indices considered in this study, and found that MPDSI can well monitor drought conditions in irrigated regions. In this sense, MPDSI can monitor the actual drought conditions under human influences such as irrigation. Besides, we also found that MPDSI can well lessen overestimation of drought conditions by PDSI in terms of drought duration and drought intensity. Therefore, we can conclude that MPDSI can be accepted in drought monitoring practice across China. It should be noted here that the idea behind development of MPDSI and also the MDPSI proposed in this study can be well referenced in drought monitoring in other regions of the globe.

1. Introduction

Drought is of stochastic nature exerting damaging impacts on human society and eco-environment. Therefore, drought is often considered as one of the costliest natural hazards of the world (Coumou and Rahmstorf, 2012; Mishra and Singh, 2010; Salinger et al., 2000; Wilhite, 2000; Wilhite, 2016; Zargar et al., 2011; Zhang et al., 2018). Drought-induced global economic losses were estimated to be as high as 6 to 8 billion US dollars each year, being far more than other meteorological disasters (Wilhite, 2000). In recent decades, growing population and expansion of agricultural, energy and industrial sectors drive the demand for water resources and even water scarcity has been occurring almost annually in many regions of the globe (Vörösmarty et al., 2000; Mishra and Singh, 2010; Sternberg, 2011). Furthermore, the well-evidenced global warming potentially triggers accelerated hydrological cycle (Allen and Ingram, 2002), and hence increased occurrences of climate extremes and subsequently increased frequency and intensity of floods and droughts can be expected in many regions of the globe (Alexander et al., 2006; Li et al., 2015; Hu et al., 2018). Sustainable development goals (SDGs) were proposed in 2015 and comprised of 17 goals and 169 targets. Droughts directly threaten food security and further affect water degradation, ecological crisis and poverty and so on (Pradhan et al., 2017). Therefore, how to deepen human knowledge of droughts and to enhance human adaptation to droughts are crucial for sustainable development of human society in a warming environment (Battisti and Naylor, 2009; He et al., 2017).

Monitoring of droughts is the first step into human adaptation and related management of drought hazards. Therefore, there stand numerous indices for drought monitoring (e.g. Zargar et al., 2011; Sun et al., 2017a). Early development of drought indices mostly focused on satellite images and remote sensing data such as precipitation in the Standardized Precipitation Index (SPI) (McKee et al., 1993) which was

* Corresponding author at: Key Laboratory of Environmental Change and Natural Disaster, Ministry of Education, Beijing Normal University, Beijing 100875, China.
E-mail address: zhangq68@bnu.edu.cn (Q. Zhang).

https://doi.org/10.1016/j.envint.2019.104951
Received 20 January 2019; Received in revised form 19 June 2019; Accepted 20 June 2019
Available online 01 July 2019

widely used in drought monitoring practice (Bonaccorso et al., 2003; Moreira et al., 2008). However, SPI index excludes impacts from temperature variations and hence Tsakiris et al. (2007) proposed Reconnaissance Drought Index (RDI) which combined hydrological and meteorological variables. In addition, Vicente-Serrano et al. (2010) proposed the Standardized Precipitation Evapotranspiration Index (SPEI) which included evapotranspiration (ET) into drought monitoring practice.

These aforementioned drought indices were developed based on in situ observed meteorological data. Recent decades witnessed more and more drought indices based on remotely sensed data such as NDVI (Normalized Difference Vegetation Index) (Rouse Jr et al., 1973), VCI (Vegetation Condition Index) (Kogan, 1990), TCI (Temperature Condition Index) (Kogan, 1995), VHI (Vegetation Health Index) (Kogan, 2001) and VTCI (Vegetation Temperature Condition Index) (Wang et al., 2001). The representative drought indices based on these remotely sensed data include CWSI (Crop Water Stress Index) (Jackson et al., 1988), TVDI (Temperature Vegetation Drought Index) (Wang et al., 2004), MPDI (Modified Perpendicular Drought Index) (Ghulam et al., 2007), MMSDI (Modified Multivariate Standardized Drought Index) (Zhang et al., 2018) and IRSDI (Integrated Remote Sensing Drought Monitoring Index) (Sun et al., 2017b). These drought indices have been widely used in agricultural drought monitoring. However, drought monitoring performance of these aforementioned drought indices heavily depends on quality of the remotely sensed data. Satellite images and remotely sensed data were used in monitoring drought indirectly by quantifying the relationship between variables obtained from remotely sensed data, such as vegetation, land surface temperature, soil moisture and so on. The NASA released MODIS products through the internet for free, which are commonly used for drought monitoring. However, it also has the disadvantage of insufficient sample size because the data began to be recorded around 2000.While, the remotely sensed data-based drought indices can well monitor droughts in a timely way over a large space scale.

Palmer (1965) developed the PDSI (Palmer Drought Severity Index) based on water balance theory considering precipitation, soil moisture, runoff and potential ET. This drought index involves clear physical mechanism and hence can be used to monitor long-term evolution of droughts. Thus, this drought index has been widely used in drought monitoring practice (Diaz, 1983; Dai et al., 2004; Dai, 2011a, 2011b, 2013; Sheffield and Wood, 2008; Sheffield et al., 2012). However, the PDSI contains a range of empirical parameters which heavily depend on regional geographical features. Therefore, the parameters should be modulated based on regional geographical features and hence spatial comparisons of PDSI-based droughts are not practically justified (Alley, 1984; Guttman et al., 1992; Karl, 1983, 1986). In this case, Wells et al. (2004) proposed the sc-PDSI (Self-Calibrating Palmer Drought Severity Index) with aim to enhance spatial comparisons of the PDSI-based droughts. Mo and Chelliah (2006) proposed a modified high resolution Palmer Drought Severity Index which was based on the 32-km North American Regional Reanalysis data, the variables such as evaporation, potential evapotranspiration, total soil moisture, soil moisture change, and runoff can be obtained directly from the RR. Many deficiencies of the original PDSI can be corrected and it can be used to monitor floods and droughts as well. As for the disadvantage that PDSI has in calculation of water deficit/surplus conditions using a two-stage bucket model, some studies used distributed hydrological models otherwise (Xu et al., 2012). A physically based Palmer Drought Severity Index (PB-PDSI) was developed by replacing the two-stage bucket water balance model in the original PDSI with the distributed hydrological model, and the results indicated that the impact of the vegetation cover change on drought was also reflected appropriately by the PB-PDSI. Another shortcoming of the Palmer Drought Severity Index (PDSI) is that this index was limited by shortage of the long-term continuous soil moisture data and the actual evapotranspiration. Yan et al. (2013) modified the PDSI based on the Soil and Water Assessment Tool (SWAT) and applied to Luanhe River basin, North China. Similarly, Liu et al. (2015) also developed a new Palmer Drought Severity Index (PDSI) variant by coupling Variable Infiltration Capacity (VIC) model with the self-calibrating PDSI. Besides, Liu et al. (2017) generated a variety of new sc-PDSI variants (denoted as SC-PDSIx) based on sc-PDSI that enable the PDSI to reflect the drought at varying time scales, which solved the shortcoming of fixed time scales. Then they evaluated the performance of SC-PDSIx by a series of comparisons with Standardized Precipitation Index (SPI), the results showed that the multi-scalar sc-PDSI could monitor droughts at different time scales.

Each individual drought index has its own strength and weakness. Therefore, there stand remarkable discrepancies in terms of drought variations in a changing climate. Dai et al. (1998) and Dai (2011a), based on PDSI, indicated amplification of droughts and showed continuously enhancing drought risks in a warming climate. Some case studies also indicated intensified drought severity and expanded drought-affected regions due to warming climate (e.g. Briffa et al., 2009; Cai et al., 2009; Wang et al., 2010). However, Sheffield and Wood, 2008; Sheffield et al., 2012) argued that little change was observed in global drought over the past 60 years due to the fact that PDSI is exaggeratedly sensitive to warming air temperature. Therefore, PDSI tends to overestimate drought severity in a warming climate because of simplified Thornthwaite algorithm in computation of ET (Sheffield et al., 2012). Zhang et al. (2016) also evidenced significant impacts of selection of Penman-Monteith and Thornthwaite algorithms on drought monitoring results. While, Dai (2011b) indicated little impacts of selection of Penman-Monteith and Thornthwaite algorithms on drought monitoring results. Besides, drought monitoring performances of PDSI and SPEI were compared and which one can better monitor the real-world droughts is still open for debate (Dai, 2011b; Vicente-Serrano et al., 2011). Therefore, right drought index is critical for monitoring and evaluation of drought events and also human adaptation to drought hazards.

PDSI is a drought index based on the supply-and-demand concept of the water balance equation (Palmer, 1965). It can reflect the mechanism of drought and which also involves the observation of soil moisture, it may be more suitable for monitoring agricultural drought than other drought indices. Ma et al. (2014) compared the moisture departure of PDSI with that of the standardized precipitation evapotranspiration index (SPEI, Vicente-Serrano et al., 2010) and found that the water deficit/surplus conditions can be well reflected by PDSI in a more reasonable way. With focus on limitations and flaws of standing drought indices, this current study aims to improve PDSI, i.e. the modified Palmer Drought Severity Index (MPDSI), by selection of the Penman-Monteith equation and also by considering inclusion of irrigation into water balance model. Besides, the empirical parameters in the MPDSI will be estimated and verified in an adaptive way based on regional geographical features of the study regions. Comparisons were done between MPDSI, SPI, SPEI, and sc-PDSI to justify drought monitoring performance of the MPDSI developed in this study. In addition, drought monitoring was done across China evidencing applicability of the MPDSI in drought monitoring across China.

2. Data

Daily precipitation data covering a period of 1951–2014 from 2474 meteorological stations across China were obtained from the National Climate Center (NCC) of China Meteorological Administration (CMA) and were analyzed in this study. This dataset contains air temperature, precipitation, relative humidity, wind velocity and land surface temperature. Quality control of the meteorological data indicated that the length of the data series of > 55 years can be found at 2016 stations, and 402 stations have data with data series length of 30–54 years (Fig. 1b, c and d). In addition, the starting time of the data series is 1960 at most stations, i.e. 2016 stations. In this case, the study time interval of this study is 1960–2014. The missing data account for < 0.01% of

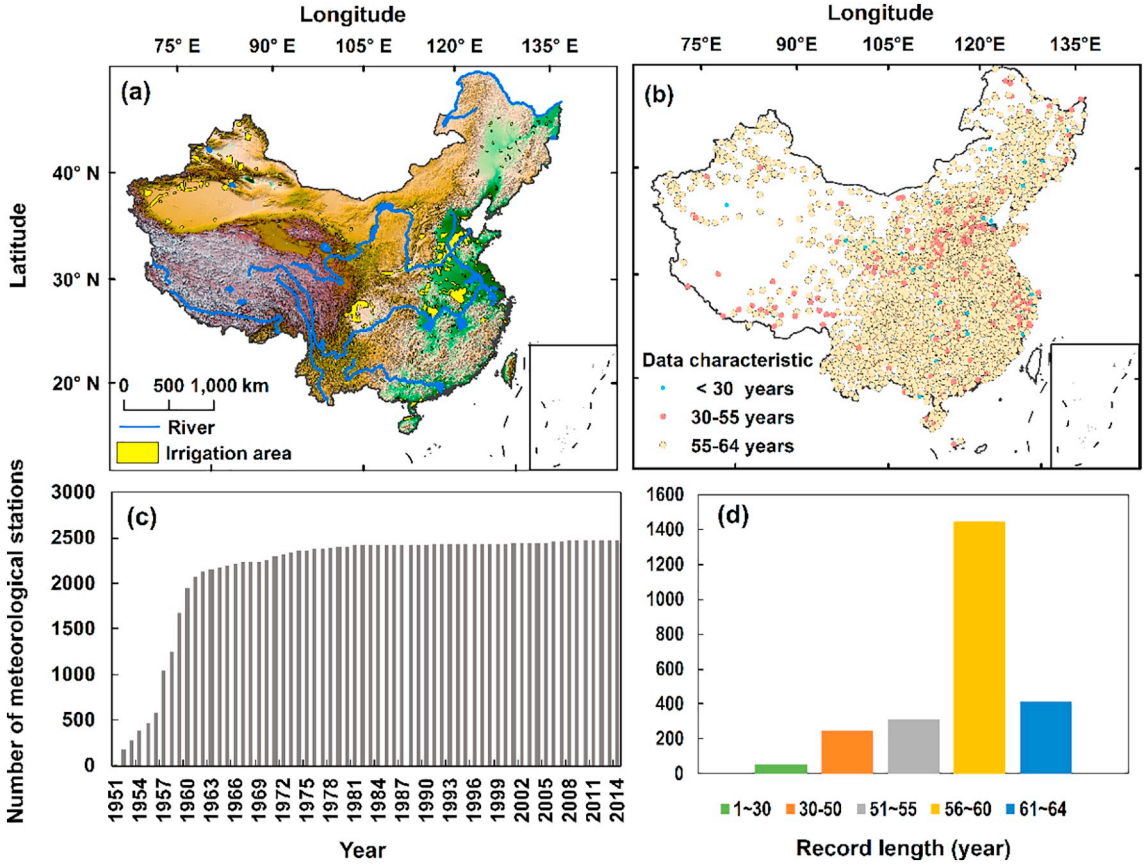

Fig. 1. Study region, meteorological stations and meteorological data. Spatial distribution of irrigation regions (a), meteorological stations and related data series length (b). Temporal distribution of the data length (c) and number of stations with different data lengths (d).

the total data. The missing data were processed based on Zhang et al. (2011). The missing values < 5 days were replaced by the average precipitation of neighboring 10 days. Adequate consecutive days with missing data were filled by the average of the same days of other three nearest meteorological stations. Available Water Capacity (AWC) reflects the soil water volume that should be available to plants, which reflects the ability of different types of soils to buffer plants during periods of moisture deficiency. The data for AWC are based on the Harmonized World Soil Database (HWSD) version 1.1 finished in March 2009 and were obtained from the data center of the Cold and Arid Regions, Chinese Academy of Science (http://westdc.westgis.ac.cn/data/tag/key/HWSD). Irrigation data were extracted from the provincial and county irrigation yearbook and the period covers 2010–2012 and the irrigation area was demonstrated in Fig. 1a.

3. Development of MPDSI

For the sake of the completeness of the computation procedure for MPDSI, here we started with the computation of PDSI which was proposed by Palmer (1965). The time scale of the PDSI is month and i denotes different months such as January, February, …, December. The letter without subscript denotes input variable for computation of PDSI. The computation of PDSI follows three steps (Fig. 2). The water deficiency, d, can be computed using water balance model.

3.1. Computation of water deficiency, d

Computation of PDSI for one specific month during one specific year will start with computation of components of water balance model based on precipitation, temperature and AWC. Then the water deficiency, d, can be obtained based on the observed precipitation and the precipitation under the Climatically Appropriate For Existing Condition (CAFEC). The computation of d should be based on components of water balance, i.e. ET, R (recharge of the real world soil moisture), RO (runoff), L (loss of the real world soil moisture), and PE (potential evaporation), PR (potential soil moisture recharge), PRO (potential runoff) and PL (potential loss of soil moisture). PET was computed based on the Thorthwaite equation (Thornthwaite, 1948). Other water balance components were obtained using the Double-Layer Soil Model (DLSM) based on real world precipitation and potential evapotranspiration.

DLSM subdivided the soil layer into two parts (Eq. (1)). Therefore, the AWC was composed by two parts, i.e. the AWC of the surface soil layer (AWC_S), being about 1 in, that is 25.4 mm; and the AWC of the underlying soil layer (AWC_U), being about 9 in, that is 228.6 mm:

$$AWC = AWC_S + AWC_U \quad (1)$$

We assume that the initial soil moisture of the surface and the underlying soil layer is respectively S_s and S_u during the early month. The soil moisture of the surface and the underlying soil layer during the first month is respectively $S_S = AWC_S$, $S_U = AWC_U$. The S_s and S_u of the other months can be computed by the real world observed soil moisture during the previous months. The largest PR the soil volume can hold is the difference between the effective soil moisture and the real world observed soil moisture (Eq. (2)):

$$PR = AWC - (S_s + S_u) \quad (2)$$

The PRO is the total soil moisture, i.e.:

$$PRO = S_s + S_u \quad (3)$$

Based on DLSM, when the precipitation is not enough for ET, the soil moisture of the surface soil layer can complement water deficiency

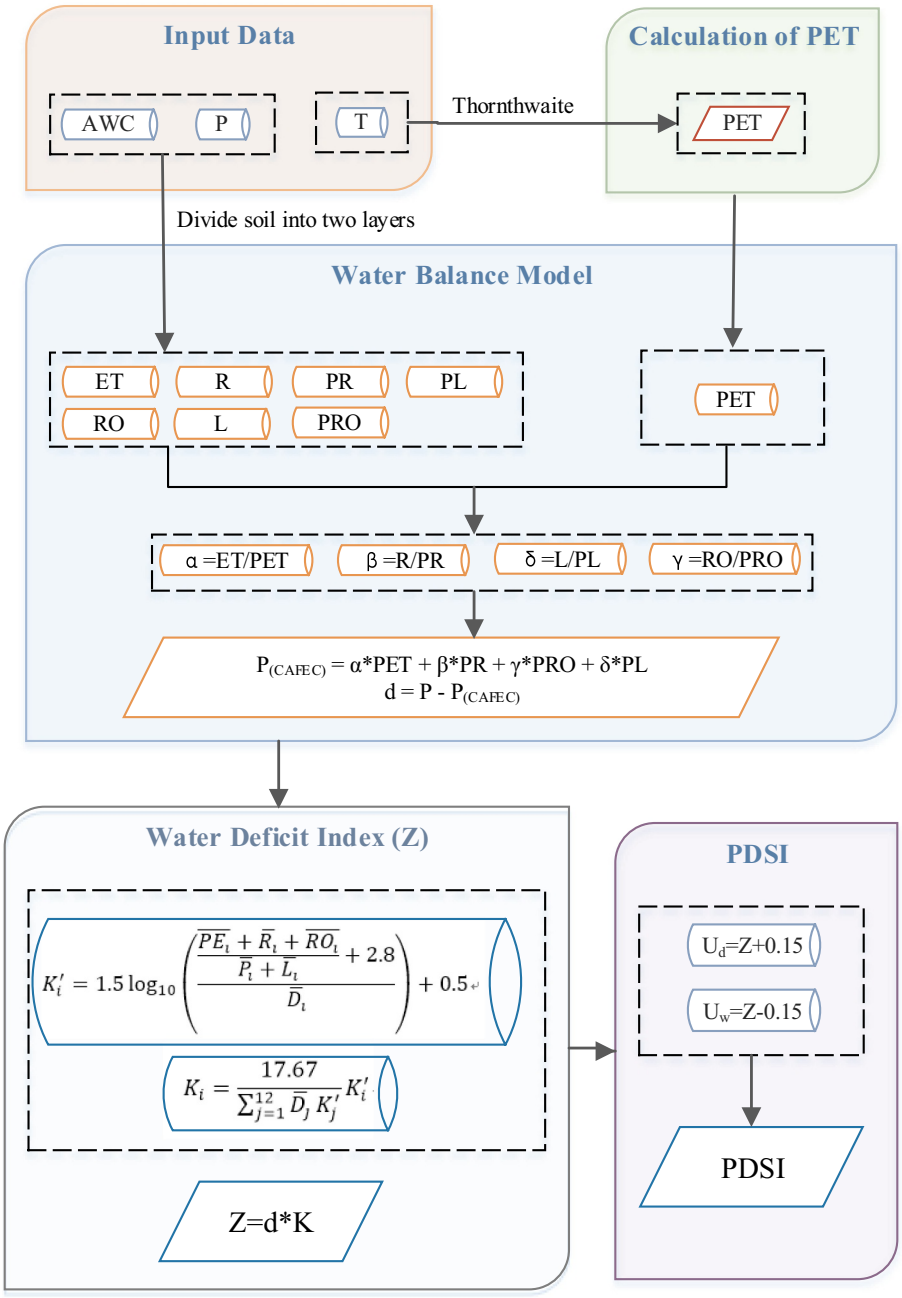

Fig. 2. Computation procedure for PDSI (Palmer Drought Severity Index).
AWC: Available Water Capacity; P: Precipitation; T: Temperature; ET: Evapotranspiration; R: Recharge; RO: Runoff; L: Loss; PET: Potential Evapotranspiration; PR: Potential Recharge; PRO: Potential Runoff; PL: Potential Loss; $P_{(CAFEC)}$: Precipitation in Climatically Appropriate For Existing Condition; D: Multi-year average of water deficient value (d); K′/K: Weighting factor; Z: Water deficit index; U_d: Effective dryness; U_w: Effective wetness.

by ET and the soil moisture of the underlying soil layer can partly satisfy ET. In this case, the PL can be obtained by the following equations:

$$PL = PL_s + PL_u \tag{4}$$

$$PL_s = min(PE,\ S_s) \tag{5}$$

$$PL_u = (PE - PL_s)\cdot\frac{S_u}{\mathrm{AWC}}\ PL_u \le S_u \tag{6}$$

The *ET*, *R*, *RO* and *L* can be computed based on *P* and *PET*: given PET ≤ P, $ET = PET$, $L = 0$, $R = 0$, $RO = P - ET - PR$; given $PET > P$, $ET = P + L$, $RO = 0$, $L = L_s + L_u$, $R = min(PE - P, PR)$. Where:

$$L_s = min(PE - P, S_s) \tag{7}$$

$$L_u = (PE - P - L_s)\cdot\frac{S_u}{\mathrm{AWC}}\ PL_u \le S_u \tag{8}$$

Based on aforementioned water balance components, the other water balance components can be obtained by:

$$\widehat{ET} = \alpha_i PE \tag{9}$$

$$\hat{R} = \beta_i PR \tag{10}$$

$$\widehat{RO} = \gamma_i PRO \tag{11}$$

$$\hat{L} = \delta_i PL \tag{12}$$

where $\alpha_i = \frac{\overline{ET_i}}{\overline{PE_i}}$, $\beta_i = \frac{\overline{R_i}}{\overline{PR_i}}$, $\gamma_i = \frac{\overline{RO_i}}{\overline{PRO_i}}$, $\delta_i = \frac{\overline{L_i}}{\overline{PL_i}}$. *i* denotes months of a year,

i.e. $i = 1, 2, 3, \ldots, 12$; α_i, β_i, γ_i, and δ_i denote coefficients of the water balance components related to ith month. Letter with straight line cap denotes mean value related to a specific month; and $\widehat{ET}$, $\widehat{R}$, $\widehat{RO}$ and $\widehat{L}$ denote respectively the ET, recharge of the soil moisture, runoff and loss of soil moisture under the CAFEC. Then we computed the precipitation amount under the CAFEC for a specific month (Eq. (14)) and also the water deficiency based on the real world observed precipitation amount (Eq. (13)):

$$d = P - \widehat{P} \tag{13}$$

$$\widehat{P} = \widehat{ET} + \widehat{R} + \widehat{RO} - \widehat{L} \tag{14}$$

where d denotes the water deficiency, P denotes the actual precipitation amount, $\widehat{P}$ denotes the precipitation amount under the CAFEC (Climatically Appropriate For Existing Condition).

3.2. Determination of Z values

The water deficiency, d, is used to measure the difference between the actual precipitation amount during the current month and the $\widehat{P}$ with unit of inch or mm. However, the $\widehat{P}$ value is different for different region and different months. Therefore, the same d value may reflect different humidity conditions given specific region and specific month, e.g. similar water deficiency may imply different drought intensities for arid and humid regions or rain and dry seasons respectively. In this case, the modification factors, K, was introduced to quantify water demand and requirement relations in a given region.

We compute water demand using $\overline{PE} + \overline{RO} + \overline{R}$ and water supply using $\overline{P} + \overline{L}$. We modified the water deficiency, d, to the water deficiency index, Z, to reflect in the right way the changes in wetness and dryness:

$$K = \frac{\text{Water demand}}{\text{Water supply}} = \frac{\overline{PE} + \overline{RO} + \overline{R}}{\overline{P} + \overline{L}} \tag{15}$$

$$Z = dK \tag{16}$$

Z index indicates the deviation of actual wetness/dryness conditions from the long term annual average water availability in a given region during a given month. In arid regions, water demand is larger than water supply and hence drought condition is higher sensitive to water deficiency or water supply than other regions. Therefore, $K > 1$ and K acts as an amplifier and emphasizes the importance of water availability, which however, does not benefit PDSI-based drought monitoring over a larger scale region. K value should be modulated again and again given drought monitoring in a specific region with specific water availability and other specific geographical properties. Later on, the K factor was further improved as shown by Eq. (17). Variable with a short line above indicates the long term annual average of this variable for a given month, i. $\overline{D_i}$ denotes the long term annual average of the absolute value of the water deficiency, d_i, during a given month, i. Hence, the modulated K value for a given region in a given month is K_i'. Comparisons done for 9 study regions indicated different $\sum \overline{D_i} K_i'$ and the average value of $\sum \overline{D_i} K_i'$ of 9 study regions, i.e. 17.67, was taken as the numerator and the $\sum \overline{D_j} K_j'$ for a given region was taken as the denominator. The K value was modulated again (Eq. (18)). The following K value can be used for drought monitoring in the study regions by Palmer only, but is not appropriate for drought monitoring in other regions than the regions by Palmer.

$$\overline{D_i} = \frac{\sum_{all\ years} |d_i|}{length\ of\ years} \tag{17}$$

$$K_i' = 1.5 \log_{10}\left(\frac{\frac{\overline{PE_i} + \overline{R_i} + \overline{RO_i}}{\overline{P_i} + \overline{L_i}} + 2.8}{\overline{D_i}} \right) + 0.5 \tag{18}$$

$$K_i = \frac{17.67}{\sum_{j=1}^{12} \overline{D_j} K_j'} K_i' \tag{19}$$

3.3. Impacts of antecedent water availability on drought conditions

Water deficiency can reflect drought intensity and drought duration is also one of the factors of drought regimes (Lee et al., 2013; Reddy and Ganguli, 2012). Considering impacts of antecedent water deficiency on drought conditions, drought duration and Z values for each individual drought event were computed to analyze impacts of antecedent water deficiency on drought intensity (Eq. (20)). The PDSI for the early stage of the drought regime can be computed by Eq. (21). The 0.897 and 1/3 are the empirical coefficients. Different equations can be obtained based on historical drought record for a given region and the empirical coefficients can be obtained correspondingly.

$$PDSI_i = 0.897 PDSI_{i-1} + \frac{1}{3} Z_i \tag{20}$$

$$PDSI_i = \frac{1}{3} Z_i \tag{21}$$

The PDSI should be determined based on the end time of a drought event. Based on classification of drought grades, $-0.5 \le \text{PDSI} \le 0.5$ means normal condition or the end of a drought event. Therefore, we have:

$$-0.5 = 0.897 PDSI_{i-1} + \frac{1}{3} Z_i \text{ given } PDSI_{i-1} < -0.5 \tag{22}$$

Taking $PDSI_{i-1} = -0.5$ into Eq. (22) indicates that the $Z_i > -0.15$ can bring end to a drought event. Therefore, the effective increase of water can be defined as:

$$U_w = Z + 0.15 \tag{23}$$

Similarly, the effective increase of aridity can be defined byU_d as:

$$0.5 = 0.897 PDSI_{i-1} + \frac{1}{3} Z_i \text{ given } PDSI_{i-1} > 0.5 \tag{24}$$

$$U_d = Z - 0.15 \tag{25}$$

The probability that the current wet or dry conditions end can be regarded as the percentage of the loss (gain) of the water volume to the loss (gain) of the water volume that actually ends the wet or dry conditions. However, it does not mean that the effective wetness and effective dryness can well replace the actual demand of water volume to end the dry conditions because a long term wet period interrupted by a dry month may also have negative impacts on effective wetness of this period, i.e. U_w. Therefore the cumulative value of the effective wetness or dryness was defined as:

If the antecedent consecutive dry condition ends, then:

$$V_i = V_{i-1} + U_w - U_w < V_{i-1} \tag{26}$$

$$V_i = 0 - U_w \ge V_{i-1} \tag{27}$$

If the antecedent consecutive wet condition ends, then:

$$V_i = V_{i-1} + U_d - U_d < V_{i-1} \tag{28}$$

$$V_i = 0 - U_d \ge V_{i-1} \tag{29}$$

And then the probability that the antecedent consecutive wet/dry condition ends can be computed as:

$$P_e = \frac{V_i}{Z_i + V_{i-1}} * 100\% \tag{30}$$

Given $P_e = 100\%$, the backtracking will be started and then the PDSI can be obtained. In the aforementioned analysis, three parameters were set, i.e. the PDSI just before the start of a wet event, the PDSI just before the start of a dry event and PDSI of the current month. The actual PDSI can be selected from these three parameters based on computed

Table 1
Classification of the Palmer Drought Severity Index (PDSI) value.

Value	Classification	Value	Classification
> 4.00	Extreme wet	−0.99 to −0.50	Slight drought
3.00–3.99	Severe wet	−1.99 to −1.00	Mild drought
2.00–2.99	Moderate wet	−2.99 to −2.00	Moderate drought
1.00–1.99	Mild wet	−3.99 to −3.00	Severe drought
0.50–0.99	Slight wet	< −4.00	Extreme drought
−0.49–0.49	Normal		

P_e. Classification of PDSI can be referred to Table 1.

3.4. Computation of sc-PDSI

The entire computation procedure of PDSI contains numerous empirical parameters and these parameters will be evaluated based on the hydrothermal conditions of the study regions. Therefore, limitations of the PDSI in regional drought monitoring are evident. Wells et al. (2004) proposed self-calibrated PDSI, i.e. sc-PDSI. The basic idea of the sc-PDSI is to decide the weighting factors and duration factors based on in situ observed hydrometeorological variables. In the analysis procedure, the self-calibrating of the empirical parameters can be done and hence the sc-PDSI enhanced spatiotemporal comparison of the drought monitoring results. More detailed algorithms and computation procedures can be found in Wells et al. (2004).

3.5. Development of the MPDSI

It was well evidenced that selections of the algorithms for ET can heavily influence the drought monitoring results by PDSI (e.g. Sheffield and Wood, 2008; Sheffield et al., 2012). PDSI with ET by Thorthwaite method is highly sensitive to temperature changes and so significant drought amplification can be expected in a warming climate given PDSI with ET by Thorthwaite method. Zhang et al. (2016) indicated higher drought intensity using PDSI with Thornthwaite method than that using PDSI with Penman-Monteith method. Therefore, it was assumed that drought intensity tended to be overestimated using PDSI with Thornthwaite method for computation of ET. In this case, we used Penman-Monteith method in evaluation of ET.

The sc-PDSI addressed calibration of empirical parameters in drought monitoring using PDSI for specific regions and this method has been widely used in global drought monitoring practice (e.g. Sheffield et al., 2012; van der Schrier et al., 2013; Osborn et al., 2016). However, computation of the precipitation amount under the CAFEC in sc-PDSI only includes *ET*, *R*, *RO*, and *L*, without considering impacts of irrigation on drought conditions, and on agricultural drought in particular. Northern China and northwestern China are the major agricultural production producers and are also heavily impacted by droughts. Irrigation is critical to maintain the agricultural production in these regions (Thomas, 2008). Therefore, irrigation and precipitation combine to act as water supplier. This constitutes the major motivation to include irrigation into MPDSI in this current study.

In this study, we include irrigation, *I*, into the modified water balance model involving precipitation, moisture variations, runoff production, loss of soil moisture, irrigation and evapotranspiration. At first, we computed the potential irrigation and component of water balance, θ_i, and then we estimated the modulated precipitation amount, $\widehat{P}$, and water deficiency, *d*, under the CAFEC, i.e.:

$$\widehat{P} = \widehat{ET} + \widehat{R} + \widehat{RO} - \widehat{L} - \widehat{I} \tag{31}$$

$$d = P - \widehat{P} \tag{32}$$

where $\theta_i = \frac{\overline{I_i}}{\overline{PI_i}}$, and $\widehat{I} = \theta_i PI$. The computation of the *PR*, *PRO*, and *PL* is the same as those for PDSI. Computation of *PET* follows the Penman-Monteith equation. The water balance analysis in this case will include irrigation, i.e.:

Given PET ≤ P + I,

$$ET = \text{PET} \tag{33}$$

$$\text{L} = 0 \tag{34}$$

$$\text{R} = 0 \tag{35}$$

$$\text{RO} = \text{P} + \text{I} - \text{ET} - \text{PR} \tag{36}$$

Given PET > P + I,

$$ET = \text{P} + \text{L} \tag{37}$$

$$\text{RO} = 0 \tag{38}$$

$$L = L_s + L_u \tag{39}$$

$$R = min(PE - P - I?PR) \tag{40}$$

wherein $L_s = min(PE - P - I,\ S_s)$; and $L_u = (PE - P - I - L_s)\cdot\frac{S_u}{\text{AWC}}$, given $PL_u \le S_u$. In this study, information pertaining to irrigation management during 2010–2012 was obtained from 172 agrometeorological stations, and the irrigation management information includes irrigation timing, irrigation amount, and so on. Based on this dataset, we decided irrigation frequency and the quota of irrigation, I_{quota}. We decided whether the irrigation is done or not based on irrigation frequency and irrigation threshold (the threshold soil moisture when irrigation is necessary). The irrigation amount, *I*, is 0 given the actual soil moisture is larger than the irrigation threshold or the irrigation times are larger than the rated irrigation times. When the soil moisture is too small to satisfy the water demand by normal plant growth, the irrigation will be done and the irrigation amount is decided by:

$$I = min(De,\ I_{quota}) \tag{41}$$

where *De* denotes the soil moisture deficiency and can be computed as:

$$\text{When } AWC - (S_s + S_u) < P,\ \text{ i. e. } PR < P,\ \text{ then } De = 0 \tag{42}$$

$$\text{When } AWC - (S_s + S_u) > P,\ \text{ i. e. } PR > P,$$
$$\text{then } De = AWC - (S_s + S_u) - P \tag{43}$$

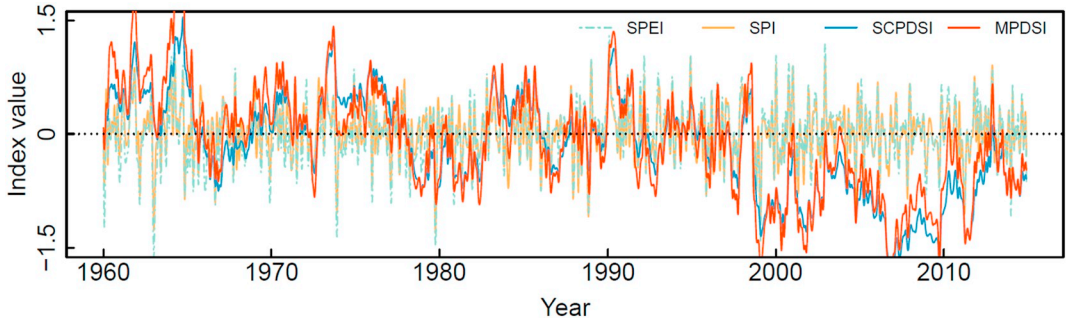

Fig. 3. Temporal variations of the SPI, SPEI, SCPDSI and MPDSI over China. SPI: Standardized Precipitation Index; SPEI: Standardized Precipitation Evapotranspiration Index; SCPDSI: self-calibrated Palmer Drought Severity Index; MPDSI: Modified Palmer Drought Severity Index.

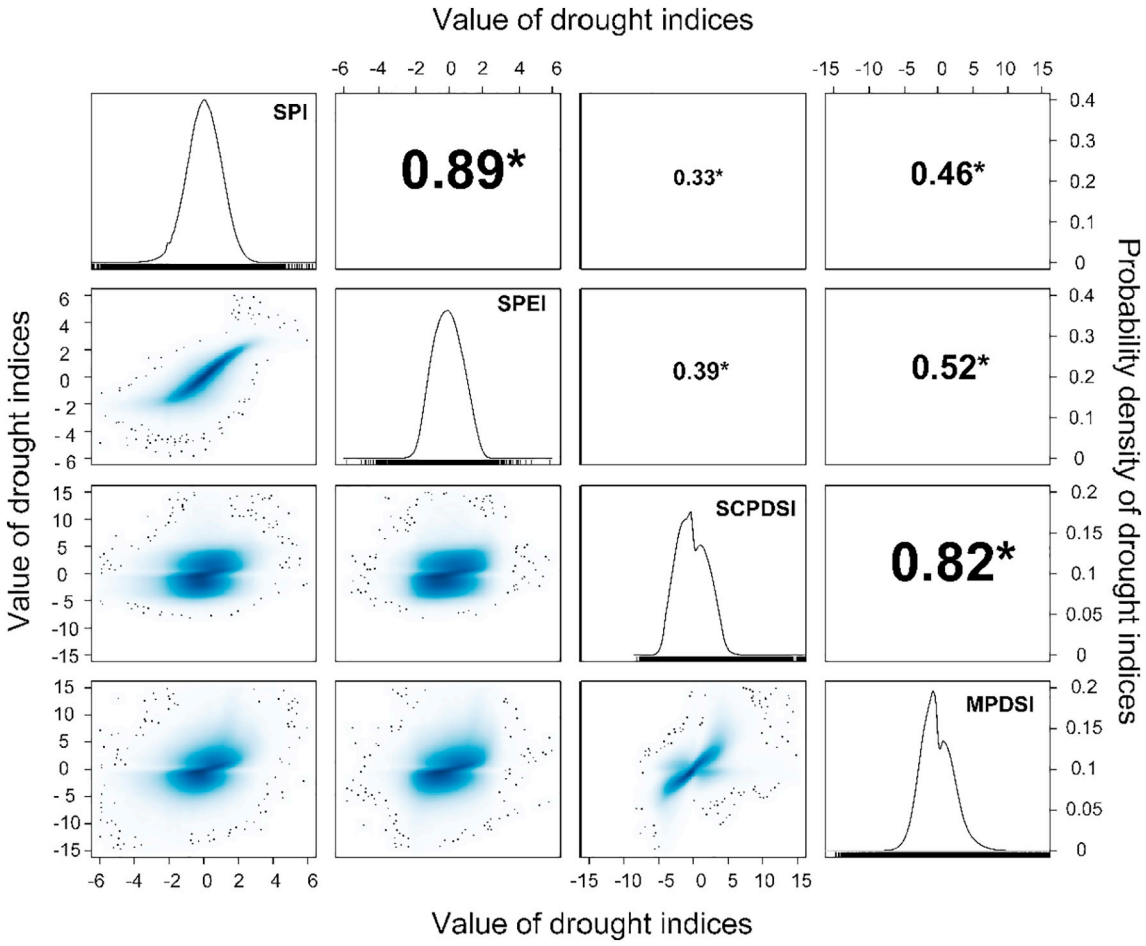

Fig. 4. Density distribution, scatter plots and correlation coefficient for drought indices considered in this study based on observations at 2474 stations across China. Insets along the diagonal direction shows the density distribution of the drought indices with x axis for drought indices and y axis for density of drought indices; the lower left triangle shows scatter plots with x axes and y axes for drought indices considered in this study; the upper right triangle shows correlations between drought indices considered in this study. * denotes the correlation is significant at 0.001 significance level. SPI: Standardized Precipitation Index; SPEI: Standardized Precipitation Evapotranspiration Index; SCPDSI: self-calibrated Palmer Drought Severity Index; MPDSI: Modified Palmer Drought Severity Index.

Table 2
Classification of the Standardized Precipitation Evapotranspiration Index (SPEI) and Standardized Precipitation Index (SPI) values.

Value	Classification	Value	Classification
≥2.00	Extreme wet	−1.00 to −0.49	Mild drought
1.50–1.99	Severe wet	−1.5 to −0.99	Moderate drought
1.00–1.49	Moderate wet	−2.00 to −1.49	Severe drought
0.5–0.99	Mild wet	< −2.00	Extreme drought
−0.5–0.49	Normal		

The relative soil moisture refers to the percentage of soil moisture content to the field capacity (%). The field capacity refers to the soil moisture content when the soil capillary water reaches the maximum, expressed as percentage by weight. The soil moisture content refers to the weight of water in the soil divided by the weight of the dry soil, expressed as percentage by weight. Taking the winter wheat as an example, the relative humidity threshold is 70% for the seedling stage, tillering period, overwintering, and greening period is 70%. The relative humidity is 80% for jointing and booting, filling time when more water is required. The relative humidity threshold for maturity is relatively smaller, being 55%.

3.6. Copula-based identification of drought events

Drought processes are in slow evolution in both space and time when compared to other extreme events such as flash floods. The entire drought processes are usually interrupted by a range of intermittent drought episodes with different drought intensities and drought durations. In this case, drought events defined by Run theory usually underestimate drought intensities (Herbst et al., 1966). Therefore, the joint functions by Copula can define drought events using different drought properties and can better identify drought events when compared to Run theory. Copula was proposed as a joint function which has been widely used in hydrological drought (Shiau et al., 2010), meteorological drought (She and Xia, 2018), and heavy rain disasters (Sarhadi et al., 2016). Shiau (2006) developed a two-dimensional joint distribution function with drought duration and drought intensity as variables. Mirabbasi et al. (2012) analyzed drought frequency during 1967–2007 using the Gumbel-copula function with the best fitting performance. The Copula function has impressive performances in modelling multivariate drought regimes. Therefore, we accepted two drought features, i.e. drought duration and drought intensity, for further analysis using Copula functions in monitoring of droughts by SPI, SPEI, sc-PDSI and MPDSI (Figs. 5, 6, and Table 3).

4. Results and discussions

We verified the drought monitoring performance of MPDSI proposed in this study. Firstly, we compared drought monitoring results by MPDSI and those by SPI, SPEI and sc-PDSI to show rationality of MPDSI when compared to standing drought monitoring indices. Besides, the advantages of the drought monitoring performance of MPDSI over the standing drought monitoring indices considered in this study were evaluated based on comparisons between the droughts monitored by the drought indices and the observed or recorded drought events and drought processes across China.

4.1. Comparison of monitored drought processes by drought indices and correlations

Fig. 3 shows the temporal variations of monthly droughts during 1960–2014 by SPI, SPEI, sc-PDSI and MPDSI respectively. The dashed line marked by 0 shows the normal condition. We found from Fig. 3 that the drought processes by four drought indices follow the similar changing pattern, which are consistent with the results of other researches (Chen and Sun, 2015; Wang et al., 2015; Wang et al., 2017; Yan et al., 2016; Zhang et al., 2016). Specifically, we found strong consistency between SPI and SPEI, and between sc-PDSI and MPDSI. Because these two groups of drought indices monitor different drought types: SPI and SPEI are mainly for meteorological droughts, and sc-PDSI and MPDSI mainly for agricultural drought. However, we can also observe similar fluctuations between SPI, SPEI, and sc-PDSI and MPDSI due to causality between meteorological and agricultural droughts in mechanisms. Besides, we found larger fluctuation magnitude in MPDSI than in sc-PDSI changes before 1980, high agreement between MPDSI and sc-PDSI changes during 1980–2000, but lower fluctuation magnitude in MPDSI than in sc-PDSI. This result implies less sensitivity of MDPSI to temperature changes than sc-PDSI. Sheffield et al. (2012) argued that PDSI tends to overestimated drought conditions in a warming climate due to excessive sensitivity of PDSI to warming temperature. Therefore, the MPDSI has the advantage over the sc-PDSI in response to warming temperature. We can expect unbiased evaluation of drought conditions in a warming climate using MPDSI.

Furthermore, we also quantitatively evaluated correlations between drought conditions monitored by four drought indices considered in this study (Fig. 4). The numbers listed in the upper right triangle of graph matrix display correlation coefficients of the drought indices, and the significance was tested at 0.001 significance level. The curves along the diagonal of the graph matrix show the density distributions of each drought index value and the lower left triangle of the graph matrix for the marginal carpet.

Correlation coefficients between SPI and SPEI, sc-PDSI and MPDSI are respectively 0.89 and 0.82, and the correlation coefficients are statistically significant. While, correlation coefficients between SPI and sc-PDSI, MPDSI are respectively 0.33 and 0.46, and are statistically

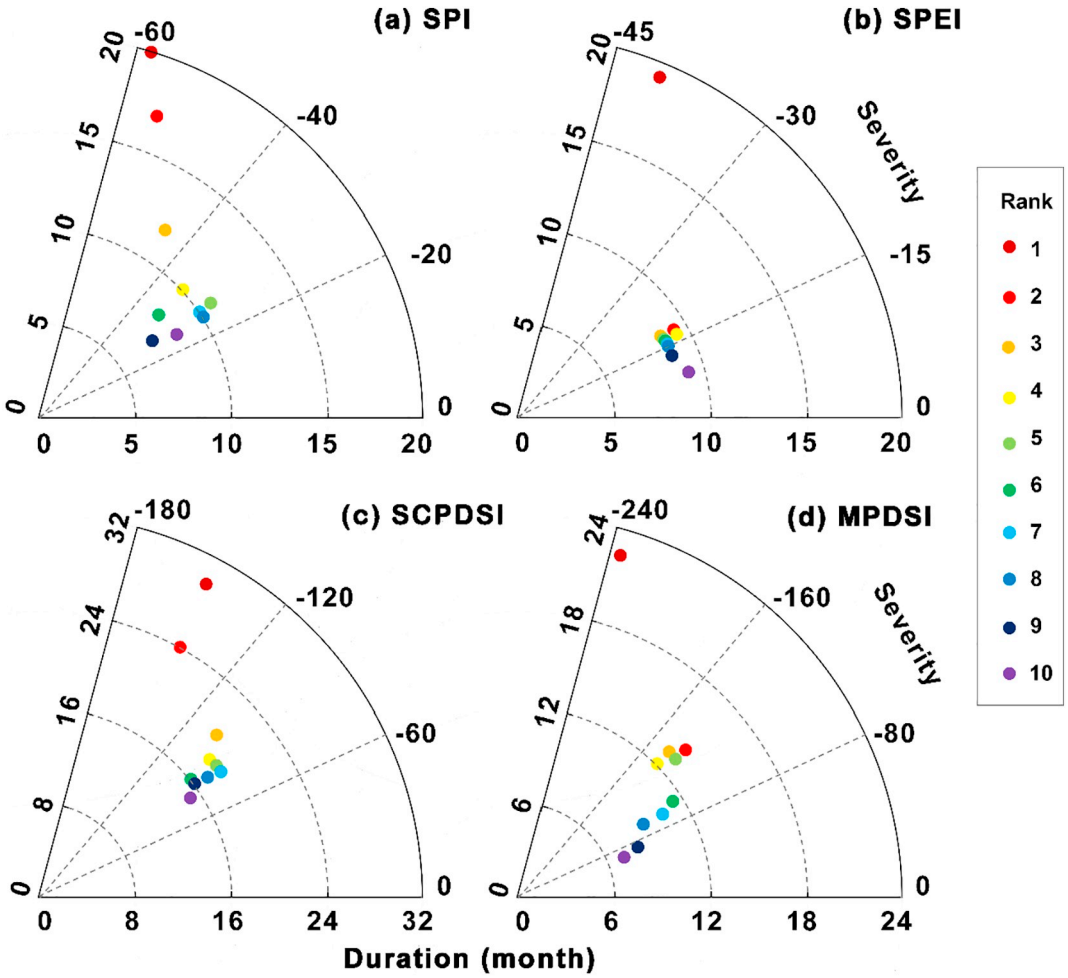

Fig. 5. Relations between duration and severity of the largest 10 drought events during 1960–2014 monitored by SPI (a), SPEI (b), SCPDSI (c) and MPDSI (d). SPI: Standardized Precipitation Index; SPEI: Standardized Precipitation Evapotranspiration Index; SCPDSI: self-calibrated Palmer Drought Severity Index; MPDSI: Modified Palmer Drought Severity Index.

Table 3
Statistical features of the 10 worst droughts during 1960–2014.

Drought index	Rank	Start	End	Duration (month)	Severity (cumulative drought index)
SPI	1	2008.09	2010.04	20	−58.1141
	2	2012.11	2014.03	17	−54.9758
	3	2006.08	2007.07	12	−46.0758
	4	2010.10	2011.07	10	−34.4566
	5	2011.07	2012.05	11	−27.5851
	6	2010.01	2010.08	8	−35.1577
	7	2014.02	2014.11	10	−27.9006
	8	2007.02	2007.11	10	−25.897
	9	2011.04	2011.10	7	−29.6136
	10	2014.01	2014.08	8	−26.9989
SPEI	1	1962.02	1963.08	19	−39.427
	2	1960.06	1961.02	9	−18.0738
	3	1961.09	1962.04	8	−18.3994
	4	2013.02	2013.10	9	−16.7941
	5	1965.05	1966.00	8	−16.3641
	6	2010.01	2010.08	8	−16.2952
	7	1970.11	1971.06	8	−16.0613
	8	2007.04	2007.11	8	−15.1269
	9	2013.11	2014.06	8	−14.3753
	10	2008.12	2009.07	8	−14.231
SCPDSI	1	2010.03	2012.08	30	−154.86
	2	2003.10	2005.09	24	−148.29
	3	1960.12	1962.07	20	−108.55
	4	1993.11	1995.04	18	−94.08
	5	1966.11	1968.04	18	−88.94
	6	2013.09	2014.12	16	−93.74
	7	1995.12	1997.05	18	−85.53
	8	2002.12	2004.04	17	−87.22
	9	1997.05	1998.08	16	−88.46
	10	1979.05	1980.07	15	−82.62
MPDSI	1	2011.07	2013.04	22	−231.3
	2	2000.07	2001.08	14	−129.6
	3	2006.07	2007.07	13	−138.03
	4	2007.06	2008.05	12	−135.88
	5	2010.06	2011.06	13	−128.7
	6	2011.08	2012.06	11	−101.44
	7	2004.09	2005.06	10	−94.15
	8	2009.07	2010.03	9	−97.7
	9	2010.06	2011.01	8	−70.6
	10	2011.01	2011.07	7	−63.41

SPI: Standardized Precipitation Index; SPEI: Standardized Precipitation Evapotranspiration Index; SCPDSI: self-calibrated Palmer Drought Severity Index; MPDSI: Modified Palmer Drought Severity Index.

significant at 0.001 significance level. This result indicates evident relations between meteorological droughts and agricultural droughts. Density distribution and carpet marginal plots indicate that values of SPI and SPEI are between −2 and 2 with maximum density value of around 0.4. However, values of sc-PDSI and MPDSI are between −4 and 4 with maximum density value of around 0.2. −2 and −4 corresponds well to the marginal threshold of the SPI, SPEI, sc-PDSI and MPDSI values (Tables 1 and 2). In this sense, MPDSI follows the classification categories of the sc-PDSI and is similar to sc-PDSI in physical sense.

4.2. Drought monitoring performance of MDPSI

In terms of drought duration, the longest duration of the 10 most serious drought events monitored by SPI and SPEI was 20 months and 19 months, respectively. However, the durations of these 10 drought events are mostly 8–10 months. (Fig. 5a and b). The longest durations of droughts monitored by sc-PDSI and MPDSI are respectively 22 months and 30 months, respectively. Meanwhile, durations of 8 out of 10 drought events monitored by sc-PDSI are mostly 15–20 months (Fig. 5c and Table 3). In addition, durations of droughts monitored by MPDSI are in good agreement with those by SPI and SPEI. From the perspective of drought duration, the durations of droughts monitored by sc-PDSI are relatively longer than those by SPI, SPEI and MPDSI. This result further corroborated the findings by Sheffield and Wood (2008); Sheffield et al. (2012) that PDSI tends to overestimated drought conditions. While, MPDSI proposed in this current study can well overcome this deficiency and performs better in describing drought features with respect to drought duration.

In terms of monitoring of drought intensity, different ranges of drought intensity by different drought indices (Fig. 4, Tables 1, 2) produced different drought intensities evaluated by SPI, SPEI and sc-PDSI, MPDSI. However, similar drought intensities can be observed for drought intensities by SPI, SPEI, and sc-PDSI and MPDSI respectively. The cumulative drought intensity by SPI is between −20 and −40; and the cumulative drought intensity by SPEI is about −15. The drought intensity monitored by SPEI is lower than that by SPI because the SPEI includes impacts of evapotranspiration on drought intensity, but not precipitation only. When compared to drought intensity by sc-PDSI, drought intensity monitored by MPDSI is lower than that by sc-PDSI. While, the cumulative drought intensity by sc-PDSI ranges between −82.62 and −154.86 and the drought duration ranges between 15 and 30 (Fig. 5 and Table 3); the cumulative drought intensity by MPDSI ranges between −63.41 and −231.3 and the drought duration ranges between 7 and 22 (Fig. 5 and Table 3). Therefore, modulations of evapotranspiration and inclusion of impacts of irrigation, drought intensities and drought durations are significantly modified to reflect the actual drought conditions.

Fig. 6 illustrates spatial evolutions of the most severe 100 drought events in terms of drought durations and drought intensity in recent 55 years across China. The size of the filled circles denotes the drought duration of the period, and the color characterizes the intensity of drought. Here the drought intensity refers to the accumulative drought intensity. Fig. 6 tells the story that droughts monitored by SPI were identified mainly in eastern China and the severe droughts in the Yellow River basin and northeastern China. While, droughts monitored by SPEI were identified mainly in northern China and specifically, the Yellow River basin and the northwestern China are the regions dominated by frequent severe droughts. The droughts monitored by sc-PDSI were observed mainly in southern China. The Yangtze River Basin and the Pearl River Basin are the regions dominated by frequent drought hazards. Droughts monitored by SPI and SPEI are mainly meteorological droughts and hence the spatial pattern of droughts by SPI and SPEI is similar. Droughts monitored by MPDSI were found mainly in the regions between the Yellow River and the Yangtze River and in the northeastern China as well. However, pretty few droughts can be found in the Xinjiang, northwestern China. It should be noted here that croplands in the Xinjiang region and in the northern China as well are well irrigated (Zhang et al., 2015). Irrigation can greatly alleviate negative impacts of droughts on agricultural production. In this current study, irrigation was included in the development of MPDSI, and hence the impacts of irrigation on drought intensity and drought duration were well considered. This is why the irrigated regions were dominated by few droughts. In this sense, MPDSI can better reflect actual drought conditions when compared to standing drought indices and SPI, SPEI, sc-PDSI in this study in particular.

Chen and Sun (2015) detected that droughts occurred more frequently and were more severe in the early twenty-first century, which is in good line with our findings about drought occurrences in the northern basins, but is not in agreement with our findings about drought occurrences in the southern river basins. It could be due to the fact that the drought index such as SPEI is more sensitive to precipitation rather than temperature. In terms of the corresponding relationship between precipitation, temperature and dry-wet change, precipitation is the critical controlling factor of dry-wet change in a region based on SPEI. Abundant rainfall in southern China will make drought monitoring weaker than actual drought conditions, which is obviously inappropriate. The results by Zhai et al. (2017) indicated that areas with a significant trend in dryness can be found in a band

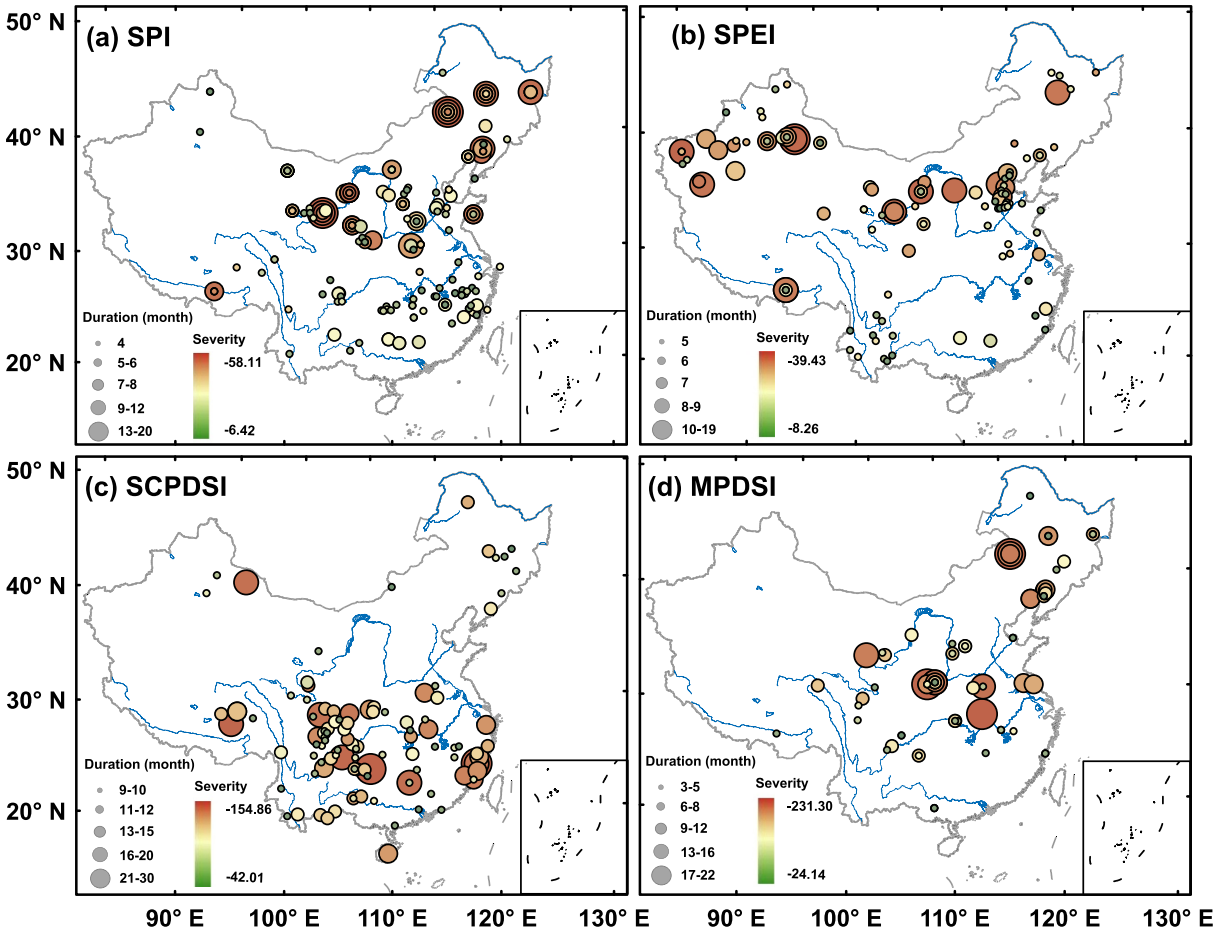

Fig. 6. Spatial distribution of the severest 100 drought events during 1960–2014 with respect to drought severity and drought duration. SPI: Standardized Precipitation Index; SPEI: Standardized Precipitation Evapotranspiration Index; SCPDSI: self-calibrated Palmer Drought Severity Index; MPDSI: Modified Palmer Drought Severity Index.

reaching in a direction from the southwest to the northeast of China, while areas with significant trends in wetness are especially detected in the northern river basins in recent decades. They monitored droughts based on SPI, which also has the shortcoming of being too sensitive to precipitation. But in their study, the relationships between the intensity and the area of droughts for a specific duration were analyzed by the intensity-area-duration method, which means that the determination of drought events not only depends on drought intensity, but also on drought duration and drought-affected area. It can overcome the deficiency of identifying drought events only through indices and reflect the actual distribution of drought events in a right way. The drought distribution proposed by Zhai et al. (2017) is obviously different from the spatial distribution of the severest 100 drought events identified by SCPDSI (Fig. 6c), which is to some extent in line with the findings about spatial distribution of the severest 100 drought events identified by MPDSI (Fig. 6d). It may be due to the fact that sc-PDSI is exaggeratedly sensitive to warming air temperature (Sheffield and Wood, 2008; Sheffield et al., 2012), while MDPSI is less sensitive to temperature changes than sc-PDSI (Fig. 3). In general, the results by Chen and Sun (2015) and Zhai et al. (2017) implied that MPDSI can be more reasonable to reflect the real droughts than other alternative drought indices.

4.3. Drought monitoring performance of MPDSI by observed droughts

Fig. 7 demonstrates the spatial pattern of the cumulative value of the drought indices across China. The filled red circles denote the center of the drought-affected regions, showing spatial evolutions of the drought regimes. In the summer of 2009, severe drought occurred in southwestern China, which continued in the following autumn and winter seasons, resulting in widespread water shortage. Zhang et al. (2013) suggested that the precipitation deficiency in 2009 was due to the emergence of the El Niño phenomenon, resulting in a large range of deficit precipitation in the southwestern China, especially higher than 50% of precipitation deficiency occurred during September 2009 to March 2010. Less precipitation and sustained high temperatures were the main driving factors behind these heavy droughts (Lu et al., 2011; Zhang et al., 2012; Yang et al., 2012). During October 2010 to February 2011, the northern China and also the main winter wheat supplier was dominated by severe droughts. During January–May 2011, drought center moved to the middle and lower Yangtze River basin. Thereafter, the drought was relieved on the arrival of the rainy season. In the following May–October, 2011, precipitation deficiency was observed in the southwestern China and was followed by severe droughts. We can find from Fig. 7 that SPEI and MPDSI can well describe spatial evolution of droughts.

Fig. 8 shows spatial distribution and spatial evolution of droughts monitored by SPI, SPEI, sc-PDSI, and MPDSI during September 2009 to April 2010. It can be seen from Fig. 8 that droughts occurred over majority of regions across China during September and October, 2009. While, intensity of droughts monitored by sc-PDSI and MPDSI is significantly higher than that by SPI and SPEI. However, in the following months, the droughts monitored by different drought indices are in evident differences. Based on drought monitoring results by SPI and SPEI, light droughts or moderate droughts occurred over sporadic regions during November–December, 2009, and March–April 2010,

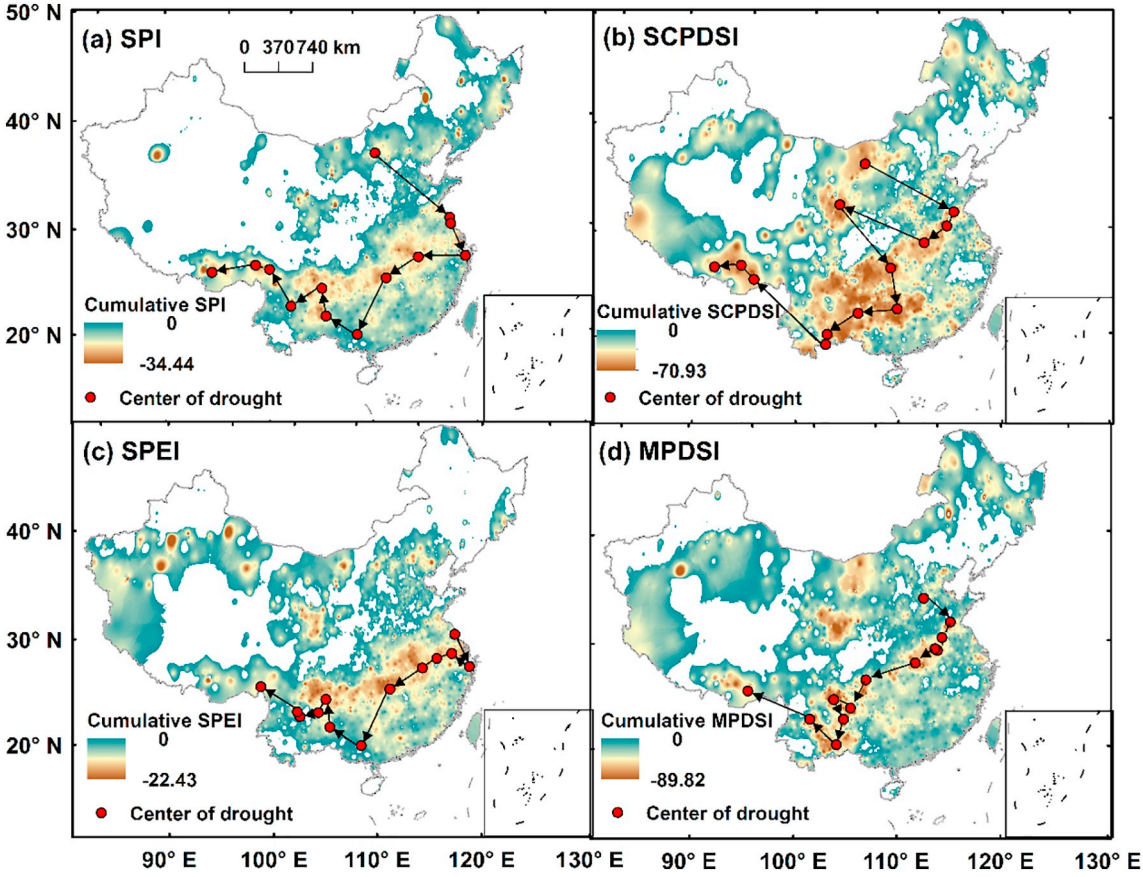

Fig. 7. Temporal and spatial drought evolution during December 2010 to December 2011.
The filled red circles denote center of drought events and the arrows denote the movement routes and related directions of the drought center. SPI: Standardized Precipitation Index; SPEI: Standardized Precipitation Evapotranspiration Index; SCPDSI: self-calibrated Palmer Drought Severity Index; MPDSI: Modified Palmer Drought Severity Index. (For interpretation of the references to color in this figure legend, the reader is referred to the web version of this article.)

which is consistent with the results by Zhao et al. (2017). These results are obviously inconsistent with the observed drought conditions. While, the drought conditions monitored by sc-PDSI and MPDSI are in good line with the observed drought conditions. Comparison of droughts monitored by sc-PDSI and MPDSI indicated similar regions dominated by droughts and the drought intensity was identical also. However, during November 2009 to April 2010, smaller regions with droughts monitored by MPDSI can be identified than sc-PDSI. Intensity of the droughts monitored by MPDSI is significantly larger than that by sc-PDSI. Observations of drought conditions indicated that the period from autumn 2009 to April 2010 witnessed 50% less precipitation than the same period of the previous years over southwestern China. Over October 2009, the droughts appeared and then expanded to the entire Yun'nan Province during November 2009. In December 2009, the droughts began to occur over Guizhou and Guangxi and started to extend to neighboring provinces. In February 2010, the droughts across the southwestern China started to intensify. It can be seen from Fig. 8 that droughts monitored by sc-PDSI reached its peak drought intensity in November 2009, and then intensified droughts were not identified based on sc-PDSI results from December 2009 to January of the subsequent year, which is inconsistent with the observed drought processes. However, drought monitoring results by the MPDSI tell another different story that intensified droughts were successfully monitored from December to April 2009 although the overall drought-affected regions were not changed significantly. Specifically, the MPDSI successfully monitored drought-affected regions such as the Yunnan and Guizhou provinces. All these results by MPDSI are in good agreement with the observed drought conditions.

5. Conclusions

Development of application of the right drought indices is the first step for appropriate drought monitoring practice. PDSI has been widely used in drought monitoring at global and regional scales. However, it was argued that PDSI tends to overestimate the drought conditions in terms of intensity and duration. In this current study, we proposed the improved version of PDSI, i.e. MPDSI, by using Penman-Monteith model for estimation of the potential evapotranspiration. Moreover, we included the irrigation into the water balance analysis and also considered the self-corrected K value to improve the PDSI index.

Although much work has been done to characterize the drought as much precision as possible, there are still some scientific issues to be answered in the ongoing investigations. Firstly, in terms of time scale, the drought indices calculated in this study are all at monthly scales which benefit the comparisons amongst drought indices. While the drought indices at weekly scale can describe the evolution process of droughts in a more specific and explicit way, and also realize calculating irrigation quota corresponding to different crop growth stages.

In addition, the growth stage of crops mostly lasts for ten days, while the time scales of drought indices are monthly. For the sake of calculation, we subdivided the entire growing period into several time intervals and roughly corresponding to different months according to the water demand in different growth stages. The calculation of the irrigation water amount is done for each month.

Thirdly, MPDSI is limited by the sample size of the irrigation data. Irrigation data is the most important factor constrainting the application of MPDSI, such as irrigation time, irrigation threshold, irrigation frequency and irrigation quota of different crops in different areas. The

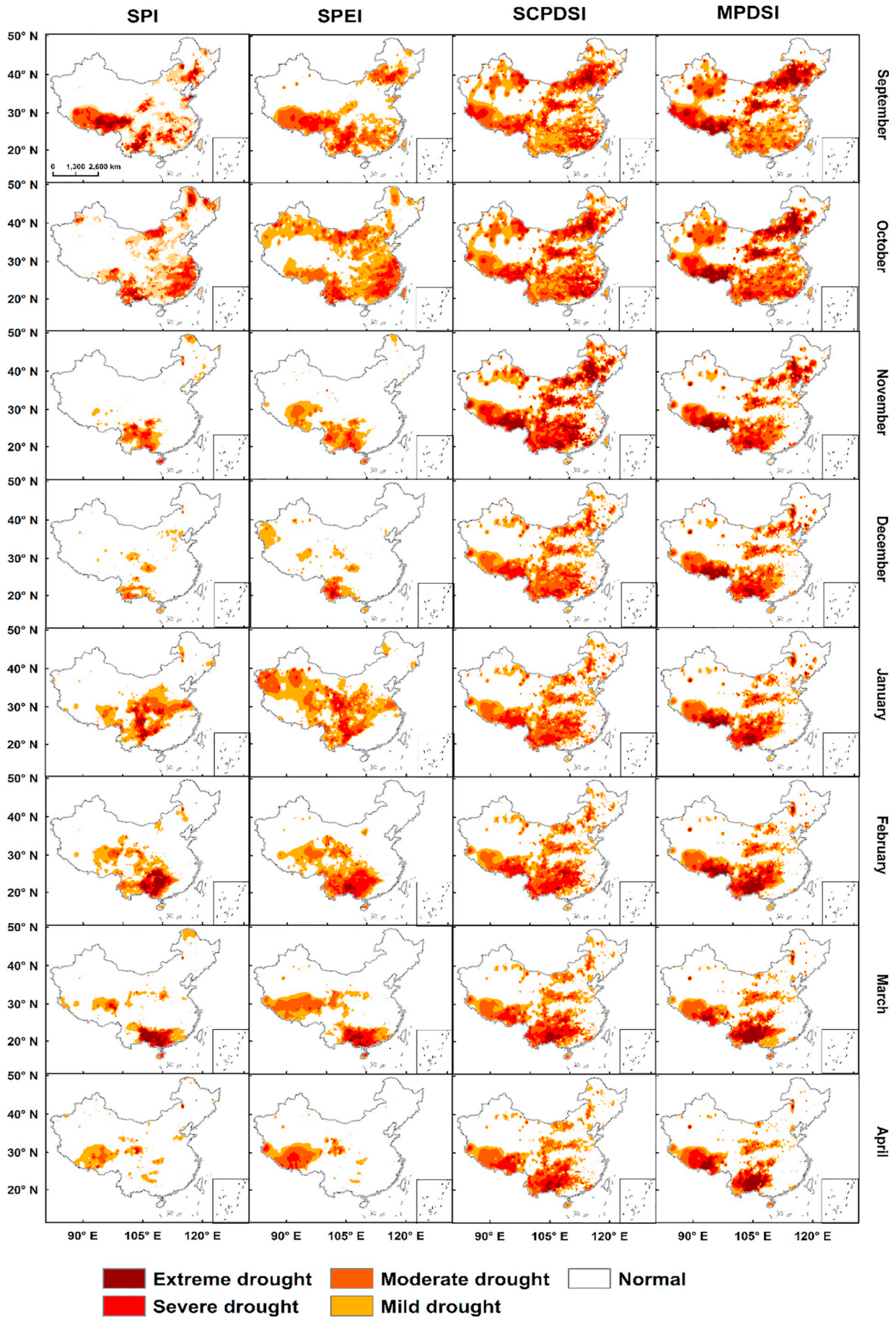

(caption on next page)

Fig. 8. Spatial patterns of droughts during September 2009 to April 2010 monitored by drought indices considered in this study, i.e. SPI, SPEI, SCPDSI, MPDSI. SPI: Standardized Precipitation Index; SPEI: Standardized Precipitation Evapotranspiration Index; SCPDSI: self-calibrated Palmer Drought Severity Index; MPDSI: Modified Palmer Drought Severity Index.

unification of time scale of the drought index and growth stages of crops, as well as better irrigation data, is conducive to quantifying the impact of irrigation on drought and enabling it more suitable for agricultural observation of irrigated areas.

Generally, the aforementioned analyses can help to obtain the following interesting and important scientific conclusions:

(1) We proposed a new version of PDSI index using Penman-Monteith model and including irrigation into water balance analysis. Comparisons between SPI, SPEI, SCPDSI and MPDSI indicated different drought monitoring results due to different physical mechanisms of each individual drought index in describing drought conditions. Besides, we further corroborated overestimation of drought conditions by PDSI. While, the MPDSI proposed in this study can well overcome this deficiency.
(2) Each drought index has its own strength and weakness in drought monitoring practice. Drought duration/drought intensity by SPEI is shorter/lower than that by SPI in that SPEI considers impacts of evapotranspiration on drought conditions. From the perspective of drought duration, the durations of droughts monitored by sc-PDSI are relatively longer than those by SPI, SPEI and MPDSI. When compared to drought intensity by sc-PDSI, drought intensity monitored by MPDSI is lower than that by sc-PDSI. In this sense, the MPDSI has advantages over PDSI and sc-PDSI in drought monitoring.
(3) Verification and evaluation of drought monitoring performance of the MDPSI indicated that droughts monitored by SPI were found mainly in the Yellow River basin and the northeastern China. Droughts monitored by SPEI were observed mainly in the northern China and in the Yellow River basin, the Xinjiang region in particular. Drought monitoring results by the sc-PDSI indicated that southern China is the regions with frequent droughts. Droughts monitored by MPDSI were found mainly in the regions between the Yellow River and the Yangtze River and in the northeastern China as well. However, few droughts can be found in the Xinjiang, northwestern China. Irrigation can greatly alleviate negative impacts of droughts and hence the impacts of irrigation on drought intensity and drought duration were well considered since that irrigation was included in the development of MPDSI.
(4) To further explore the applicability of the MPDSI method in drought monitoring across China, comparison was done on drought monitoring performance of SPI, SPEI, SCPDSI and MPDSI when compared to the observed drought processes during 2010–2011 and 2009–2010. The droughts monitored by MPDSI are consistent with the actual drought observations in terms of drought-affected area and spatial drought evolution. Therefore, we can conclude that MPDSI can be accepted in drought monitoring practice across China. Ongoing work will be focused on impacts of irrigation on drought conditions at finer time scales such as weekly and even daily time scales. Besides, different water requirements of crops during different growing seasons should also be considered in development of drought index. However, all these improvements should rely on field observations of relations between irrigation and crop growing processes.

Declaration of Competing Interest

All the authors declared no conflict of interest.

Acknowledgments

This work is financially supported by the National Science Foundation for Distinguished Young Scholars of China (Grant No. 51425903), the Fund for Creative Research Groups of National Natural Science Foundation of China (Grant No.: 41621061), National Natural Science Foundation of China (No. 41771536). Our cordial gratitude should be extended to the editor, Prof. Dr. Xavier Querol, and three anonymous reviewers for their professional and pertinent comments and thoughtful revision suggestions which are greatly helpful for further quality improvement of the current manuscript.

References

Alexander, L.V., Zhang, X., Peterson, T.C., Caesar, J., Gleason, B., Klein Tank, A.M.G., Haylock, M., Collins, D., Trewin, B., Rahimzadeh, F., Tagipour, A., Rupa Kumar, K., Revadekar, J., Griffiths, G., Vincent, L., Stephenson, D.B., Burn, J., Aguilar, E., Brunet, M., Taylor, M., New, M., Zhai, P., Rusticucci, M., Vazquez-Aguirre, J.L., 2006. Global observed changes in daily climate extremes of temperature and precipitation. Journal of Geophysical Research: Atmospheres 111 (D5). https://doi.org/10.1029/2005JD006290.
Allen, M.R., Ingram, W.J., 2002. Constraints on future changes in climate and the hydrologic cycle. Nature 419 (6903), 224–232.
Alley, W.M., 1984. The Palmer drought severity index: limitations and assumptions. J. Clim. Appl. Meteorol. 23 (7), 1100–1109.
Battisti, D.S., Naylor, R.L., 2009. Historical warnings of future food insecurity with unprecedented seasonal heat. Science 323 (5911), 240–244.
Bonaccorso, B., Bordi, I., Cancelliere, A., Rossi, G., Sutera, A., 2003. Spatial variability of drought: an analysis of the SPI in Sicily. Water Resour. Manag. 17 (4), 273–296.
Briffa, K.R., Van Der Schrier, G., Jones, P.D., 2009. Wet and dry summers in Europe since 1750: evidence of increasing drought. Int. J. Climatol. 29 (13), 1894–1905.
Cai, W., Cowan, T., Briggs, P., Raupach, M., 2009. Rising temperature depletes soil moisture and exacerbates severe drought conditions across southeast Australia. Geophys. Res. Lett. 36 (21). https://doi.org/10.1029/2009GL040334.
Chen, H., Sun, J., 2015. Changes in drought characteristics over China using the standardized precipitation evapotranspiration index. J. Clim. 28 (13), 5430–5447.
Coumou, D., Rahmstorf, S., 2012. A decade of weather extremes. Nat. Clim. Chang. 2 (7), 491–496.
Dai, A., 2011a. Drought under global warming: a review. Wiley Interdiscip. Rev. Clim. Chang. 2 (1), 45–65.
Dai, A., 2011b. Characteristics and trends in various forms of the Palmer Drought Severity Index during 1900–2008. Journal of Geophysical Research: Atmospheres 116 (D12). https://doi.org/10.1029/2010JD015541.
Dai, A., 2013. Increasing drought under global warming in observations and models. Nat. Clim. Chang. 3 (1), 52–58.
Dai, A., Trenberth, K.E., Karl, T.R., 1998. Global variations in droughts and wet spells: 1900–1995. Geophys. Res. Lett. 25 (17), 3367–3370.
Dai, A., Trenberth, K.E., Qian, T., 2004. A global dataset of Palmer Drought Severity Index for 1870–2002: relationship with soil moisture and effects of surface warming. J. Hydrometeorol. 5 (6), 1117–1130.
Diaz, H.F., 1983. Drought in the United States. J. Clim. Appl. Meteorol. 22 (1), 3–16.
Ghulam, A., Qin, Q., Teyip, T., Li, Z.L., 2007. Modified perpendicular drought index (MPDI): a real-time drought monitoring method. ISPRS J. Photogramm. Remote Sens. 62 (2), 150–164.
Guttman, N.B., Wallis, J.R., Hosking, J.R.M., 1992. Spatial comparability of the Palmer Drought Severity Index. J. Am. Water Resour. Assoc. 28 (6), 1111–1119.
He, X., Wada, Y., Wanders, N., Sheffield, J., 2017. Human water management intensifies hydrological drought in California. Geophys. Res. Lett. 1–19. https://doi.org/10.1002/2016GL071665.
Herbst, P.H., Bredenkamp, D.B., Barker, H.M.G., 1966. A technique for the evaluation of drought from rainfall data. J. Hydrol. 4 (66), 264–272.
Hu, P., Zhang, Q., Shi, P., Chen, B., Fang, J., 2018. Flood-induced mortality across the globe: spatiotemporal pattern and influencing factors. Sci. Total Environ. 643, 171–182.
Jackson, R.D., Kustas, W.P., Choudhury, B.J., 1988. A reexamination of the crop water stress index. Irrig. Sci. 9 (4), 309–317.
Karl, T.R., 1983. Some spatial characteristics of drought duration in the United States. J. Clim. Appl. Meteorol. 22 (8), 1356–1366.
Karl, T.R., 1986. The sensitivity of the Palmer drought severity index and Palmer's Z-index to their calibration coefficients including potential evapotranspiration. J. Clim. Appl. Meteorol. 25 (1), 77–86.
Kogan, F.N., 1990. Remote sensing of weather impacts on vegetation in non-homogeneous areas. Int. J. Remote Sens. 11 (8), 1405–1419.
Kogan, F.N., 1995. Application of vegetation index and brightness temperature for drought detection. Adv. Space Res. 15 (11), 91–100.
Kogan, F.N., 2001. Operational space technology for global vegetation assessment. Bull.

Am. Meteorol. Soc. 82 (9), 1949–1964.
Lee, T., Modarres, R., Ouarda, T.B., 2013. Data-based analysis of bivariate copula tail dependence for drought duration and severity. Hydrol. Process. 27 (10), 1454–1463.
Li, J., Zhang, Q., Chen, Y.D., Singh, V.P., 2015. Future joint probability behaviors of precipitation extremes across China: spatiotemporal patterns and implications for flood and drought hazards. Glob. Planet. Chang. 124, 107–122.
Liu, Y., Yang, X., Ren, L., Yuan, F., Jiang, S., Ma, M., 2015. A new physically based self-calibrating Palmer drought severity index and its performance evaluation. Water Resour. Manag. 29 (13), 4833–4847.
Liu, Y., Zhu, Y., Ren, L., Singh, V.P., Yang, X., Yuan, F., 2017. A multiscalar Palmer drought severity index. Geophys. Res. Lett. 44 (13), 6850–6858.
Lu, E., Luo, Y., Zhang, R., Wu, Q., Liu, L., 2011. Regional atmospheric anomalies responsible for the 2009–2010 severe drought in China. Journal of Geophysical Research: Atmospheres 116 (D21). https://doi.org/10.1029/2011JD015706.
Ma, M., Ren, L., Yuan, F., Jiang, S., Liu, Y., Kong, H., Gong, L., 2014. A new standardized Palmer drought index for hydro-meteorological use. Hydrol. Process. 28 (23), 5645–5661.
McKee, T.B., Doesken, N.J., Kleist, J., 1993. The relationship of drought frequency and duration to time scales. In: Proceedings of the 8th Conference on Applied Climatology, pp. 179–183 17(22).
Mirabbasi, R., Fakheri-Fard, A., Dinpashoh, Y., 2012. Bivariate drought frequency analysis using the copula method. Theor. Appl. Climatol. 108 (1–2), 191–206.
Mishra, A.K., Singh, V.P., 2010. A review of drought concepts. J. Hydrol. 391 (1–2), 202–216.
Mo, K.C., Chelliah, M., 2006. The modified Palmer drought severity index based on the NCEP North American Regional Reanalysis. J. Appl. Meteorol. Climatol. 45 (10), 1362–1375.
Moreira, E.E., Coelho, C.A., Paulo, A.A., Pereira, L.S., Mexia, J.T., 2008. SPI-based drought category prediction using log linear models. J. Hydrol. 354 (1–4), 116–130.
Osborn, T., Barichivich, J., Harris, I., Van Der Schrier, G., Jones, P., 2016. Monitoring global drought using the self-calibrating Palmer Drought Severity Index [in "State of the Climate in 2015"]. Bull. Am. Meteorol. Soc. 97, S32–S36.
Palmer, W.C., 1965. Meteorological drought. In: US Weather Bureau Research Paper. 45.
Pradhan, P., Costa, L., Rybski, D., Lucht, W., Kropp, J.P., 2017. A systematic study of Sustainable Development Goal (SDG) interactions. Earth's Future 5 (11), 1169–1179.
Reddy, M.J., Ganguli, P., 2012. Application of copulas for derivation of drought severity–duration–frequency curves. Hydrol. Process. 26 (11), 1672–1685.
Rouse Jr., J.W., Haas, R.H., Schell, J.A., Deering, D.W., 1973. Monitoring the vernal advancement and retrogradation (green wave effect) of natural vegetation. https://ntrs.nasa.gov/archive/nasa/casi.ntrs.nasa.gov/19730017588.pdf.
Salinger, M.J., Stigter, C.J., Das, H.P., 2000. Agrometeorological adaptation strategies to increasing climate variability and climate change. Agric. For. Meteorol. 103 (1–2), 167–184.
Sarhadi, A., Burn, D.H., Wiper, M.P., 2016. Time varying nonstationary multivariate risk analysis using a dynamic Bayesian copula. Water Resour. Res. 52 (3), 2327–2349.
She, D., Xia, J., 2018. Copulas-based drought characteristics analysis and risk assessment across the loess plateau of China. Water Resour. Manag. 32 (56), 1–18.
Sheffield, J., Wood, E.F., 2008. Projected changes in drought occurrence under future global warming from multi-model, multi-scenario, IPCC AR4 simulations. Clim. Dyn. 31 (1), 79–105.
Sheffield, J., Wood, E.F., Roderick, M.L., 2012. Little change in global drought over the past 60 years. Nature 491 (7424), 435–438.
Shiau, J.T., 2006. Fitting drought duration and severity with two-dimensional copulas. Water Resour. Manag. 20 (5), 795–815.
Shiau, J.T., Feng, S., Nadarajah, S., 2010. Assessment of hydrological droughts for the yellow river, China, using copulas. Hydrol. Process. 21 (16), 2157–2163.
Sternberg, T., 2011. Regional drought has a global impact. Nature 472 (7342), 169.
Sun, P., Zhang, Q., Cheng, C., Singh, V.P., Shi, P., 2017a. ENSO-induced drought hazards and wet spells and related agricultural losses across Anhui province, China. Nat. Hazards 89 (2), 963–983.
Sun, P., Zhang, Q., Wen, Q., Singh, V.P., Shi, P., 2017b. Multisource data-based integrated agricultural drought monitoring in the Huai River basin, China. Journal of Geophysical Research: Atmospheres 122 (20). https://doi.org/10.1002/2017JD027186.
Thomas, A., 2008. Agricultural irrigation demand under present and future climate scenarios in China. Glob. Planet. Chang. 60 (3), 306–326.
Thornthwaite, C.W., 1948. An approach toward a rational classification of climate. Geogr. Rev. 38 (1), 55–94.
Tsakiris, G., Pangalou, D., Vangelis, H., 2007. Regional drought assessment based on the Reconnaissance Drought Index (RDI). Water Resour. Manag. 21 (5), 821–833.
van der Schrier, G., Barichivich, J., Briffa, K.R., Jones, P.D., 2013. A scPDSI-based global data set of dry and wet spells for 1901–2009. Journal of Geophysical Research: Atmospheres 118 (10), 4025–4048.
Vicente-Serrano, S.M., Beguería, S., López-Moreno, J.I., 2010. A multi scalar drought index sensitive to global warming: the standardized precipitation evapotranspiration index. J. Clim. 23 (7), 1696–1718.
Vicente-Serrano, S.M., Beguería, S., López-Moreno, J.I., 2011. Comment on "Characteristics and trends in various forms of the Palmer Drought Severity Index (PDSI) during 1900–2008" by Aiguo Dai. Journal of Geophysical Research: Atmospheres 116 (D19). https://doi.org/10.1029/2010JD015541.
Vörösmarty, C.J., Green, P., Salisbury, J., Lammers, R.B., 2000. Global water resources: vulnerability from climate change and population growth. Science 289 (5477), 284–288.
Wang, P.X., Li, X.W., Gong, J.Y., Song, C., 2001. Vegetation temperature condition index and its application for drought monitoring. In: Geoscience and Remote Sensing Symposium, 2001. IGARSS'01. IEEE 2001 International. Vol. 1. IEEE, pp. 141–143. https://doi.org/10.1109/IGARSS.2001.976083.
Wang, C., Qi, S., Niu, Z., Wang, J., 2004. Evaluating soil moisture status in China using the temperature–vegetation dryness index (TVDI). Can. J. Remote. Sens. 30 (5), 671–679.
Wang, J., Chen, F., Jin, L., Bai, H., 2010. Characteristics of the dry/wet trend over arid central Asia over the past 100 years. Clim. Res. 41 (1), 51–59.
Wang, W., Zhu, Y., Xu, R., Liu, J., 2015. Drought severity change in China during 1961–2012 indicated by SPI and SPEI. Nat. Hazards 75 (3), 2437–2451.
Wang, Z., Li, J., Lai, C., Zeng, Z., Zhong, R., Chen, X., Zhou, X., Wang, M., 2017. Does drought in China show a significant decreasing trend from 1961 to 2009? Sci. Total Environ. 579, 314–324.
Wells, N., Goddard, S., Hayes, M.J., 2004. A self-calibrating Palmer drought severity index. J. Clim. 17 (12), 2335–2351.
Wilhite, D.A., 2000. Drought as a natural hazard: concepts and definitions. In: Drought: A Global Assessment. vol. I. pp. 3–18 chapter 1.
Wilhite, D.A., 2016. Droughts: A Global Assessment. Routledge, London (752pp).
Xu, J., Ren, L.L., Ruan, X.H., Liu, X.F., Yuan, F., 2012. Development of a physically based PDSI and its application for assessing the vegetation response to drought in northern China. Journal of Geophysical Research: Atmospheres 117 (D8). https://doi.org/10.1029/2011JD016807.
Yan, D., Shi, X., Yang, Z., Li, Y., Zhao, K., Yuan, Y., 2013. Modified palmer drought severity index based on distributed hydrological simulation. Math. Probl. Eng. 2013. https://doi.org/10.1155/2013/327374.
Yan, H., Wang, S.Q., Wang, J.B., Lu, H.Q., Guo, A.H., Zhu, Z.C., Ranga, B.M., Shugart, H.H., 2016. Assessing spatiotemporal variation of drought in China and its impact on agriculture during 1982–2011 by using PDSI indices and agriculture drought survey data. Journal of Geophysical Research: Atmospheres 121 (5), 2283–2298.
Yang, J., Gong, D., Wang, W., Hu, M., Mao, R., 2012. Extreme drought event of 2009/2010 over southwestern China. Meteorog. Atmos. Phys. 115 (3–4), 173–184.
Zargar, A., Sadiq, R., Naser, B., Khan, F.I., 2011. A review of drought indices. Environ. Rev. 19, 333–349.
Zhai, J., Huang, J., Su, B., Cao, L., Wang, Y., Jiang, T., Fischer, T., 2017. Intensity–area–duration analysis of droughts in China 1960–2013. Clim. Dyn. 48 (1–2), 151–168.
Zhang, Q., Singh, V.P., Li, J., Chen, X., 2011. Analysis of the periods of maximum consecutive wet days in China. Journal of Geophysical Research: Atmospheres 116 (D23). https://doi.org/10.1029/2011JD016088.
Zhang, L., Xiao, J., Li, J., Wang, K., Lei, L., Guo, H., 2012. The 2010 spring drought reduced primary productivity in southwestern China. Environ. Res. Lett. 7 (4). https://doi.org/10.1088/1748-9326/7/4/045706.
Zhang, W., Jin, F.F., Zhao, J.X., Qi, L., Ren, H.L., 2013. The possible influence of a nonconventional El Niño on the severe autumn drought of 2009 in Southwest China. J. Clim. 26 (21), 8392–8405.
Zhang, Q., Gu, X., Singh, V.P., Kong, D., Chen, X., 2015. Spatiotemporal behavior of floods and droughts and their impacts on agriculture in China. Glob. Planet. Chang. 131, 63–72.
Zhang, J., Sun, F., Xu, J., Chen, Y., Sang, Y.F., Liu, C., 2016. Dependence of trends in and sensitivity of drought over China (1961–2013) on potential evaporation model. Geophys. Res. Lett. 43 (1), 206–213.
Zhang, Q., Li, Q., Singh, V.P., Shi, P., Huang, Q., Sun, P., 2018. Nonparametric integrated agrometeorological drought monitoring: model development and application. Journal of Geophysical Research: Atmospheres 123 (1), 73–88.
Zhao, H., Gao, G., An, W., Zou, X., Li, H., Hou, M., 2017. Timescale differences between SC-PDSI and SPEI for drought monitoring in China. Physics and Chemistry of the Earth, Parts A/B/C 102, 48–58.